Anal. Chem. **2006,** *78,* 4803−4810

Plug−Plug Kinetic Capillary Electrophoresis: Method for Direct Determination of Rate Constants of Complex Formation and Dissociation

Victor Okhonin, Alexander P. Petrov, Maxim Berezovski, and Sergey N. Krylov*

Department of Chemistry, York University, Toronto, Ontario M3J 1P3, Canada

We present a method for direct determination of rate constants of complex formation, k_{on}, and dissociation, k_{off}. The method is termed plug−plug kinetic capillary electrophoresis (ppKCE). To explain the concept of the method, we consider the formation of a noncovalent complex C between molecules A and B; A is assumed to migrate slower in electrophoresis than B. In ppKCE, a short plug of A is injected into a capillary, followed by a short plug of B. When a high voltage is applied, the electrophoretic zone of B moves through that of A, allowing for the formation of C. When the zones of A and B are separated, C starts dissociating. The features of the resulting electropherogram are defined by both binding and dissociation. We developed a unique mathematical approach that allows finding k_{on} and k_{off} from a single electropherogram without nonlinear regression analysis. The approach uses algebraic functions with the only input parameters from electropherograms being areas and migration times of electrophoretic peaks. In this work, we explain theoretical bases of ppKCE and prove the principle of the method by finding k_{on} and k_{off} for a protein−ligand complex. The unique capability of the method to directly determine both k_{on} and k_{off} along with its simplicity make ppKCE highly attractive to a broad community of molecular scientists.

Noncovalent molecular interactions play a key role in all regulatory biological processes; for example, cell recognition, immune response, signal transduction, gene expression, DNA replication, and others.[1] Finding molecules capable of noncovalently binding therapeutic targets is the principle approach in modern drug development.[2] Furthermore, many analytical techniques and devices used in research and disease diagnostics (e.g., immunoassays, biosensors, and DNA hybridization analysis) are based on the formation of noncovalent molecular complexes.[3] Hence, efficient methods for studying noncovalent interactions are pivotal to our progress in many areas of modern physical and life sciences.

The formation and dissociation of a noncovalent complex C between molecules A and B are characterized by a bimolecular rate constant k_{on}, and a unimolecular rate constant, k_{off}, of the forward and reverse reactions, respectively.

$$A + B \underset{k_{off}}{\overset{k_{on}}{\rightleftharpoons}} C \qquad (1)$$

Knowledge of k_{on} and k_{off} is essential for (i) understanding the dynamics of biological processes, (ii) determining the pharmacokinetics of target-binding drugs, and (iii) designing quantitative affinity analyses. To the best of our knowledge, until now, there has been no method capable of directly measuring both k_{on} and k_{off} in a single experiment.

A conventional method for directly finding k_{on} is stopped-flow spectroscopy.[4] In stopped-flow spectroscopy, A and B are mixed rapidly by a stopped flow, and the change of spectral properties of either A or B during complex formation are followed. Such changes are typically insignificant, which limits the applicability of stopped-flow spectroscopy to studies of noncovalent interactions.

A conventional approach for finding k_{off} is surface plasmon resonance (SPR).[5] In SPR, A is affixed to a sensor while B is dissolved in a solution and can bind the immobilized A. The sensor changes its optical signal upon B's binding to A. To determine k_{off}, A is reacted with B to form C on the surface, and then the solution of B is quickly replaced with a buffer devoid of B. The complex on the surface dissociates in the absence of B in the solution, and the complex dissociation generates an exponential signal on the sensor. SPR can be also used to find the equilibrium constant of complex dissociation, K_d, in a series of equilibrium experiments. Due to its heterogeneous nature and poorly defined surface density of A, SPR is difficult to use for direct k_{on} determination. However, k_{on} can be calculated if both k_{off} and K_d are known: $k_{on} = k_{off}/K_d$. SPR has a number of inherent limitations. First, affixing A to the surface changes the structure of A and, thus, can potentially affect binding parameters between A and B. Second, nonspecific interactions with the surface can introduce errors into binding parameters. Third, the surface density of A, which is adsorbed to the surface, is difficult to

(1) Davis, S.; Davies, E.; Tucknott, M.; Jones, E.; van der Merwe, P. *Proc. Natl. Acad. Sci. U.S.A.* **1998**, *95*, 5490−5494.
(2) Newman-Tancredi, A.; Assie, M.; Leduc, N.; Ormiere, A.; Danty, N.; Cosi, C., *Int. J. Neuropsychopharmacol.* **2005**, *8*, 341−356.
(3) Yu, D.; Blankert, B.; Vire, J.; Kauffmann, J. *Anal. Lett.* **2005**, *38*, 1687−1701.
(4) Iakoucheva, L.; Walker, R.; van Houten, B.; Ackerman, E. *Biochemistry* **2002**, *41*, 131−143.
(5) Zanier, K.; Charbonnier, S.; Baltzinger, M.; Nomine, Y.; Altschuh, D.; Trave, G. *J. Mol. Biol.* **2005**, *349*, 401−412.

10.1021/ac060108i CCC: $33.50
Published on Web 05/26/2006

measure accurately. Finally, the immobilization procedure can be time-consuming, labor-intensive, and expensive.

In the last 3 years, we have focused on capillary electrophoresis-based kinetic methods for studies of noncovalent molecular interactions. These efforts are based on the insight that if A is allowed to interact with B during electrophoresis, the resulting electropherograms will have a memory of this interaction. Thus, we concentrated on defining different ways of interaction and developing approaches to retrieving kinetic parameters from electropherograms. We term this area of research kinetic capillary electrophoresis (KCE) and define KCE as CE separation of species that interact during electrophoresis.

To date, we described in detail two KCE methods with simplified mathematical analysis: nonequilibrium capillary electrophoresis of equilibrium mixtures (NECEEM), and sweeping capillary electrophoresis (SweepCE). NECEEM was introduced as the only method that can facilitate direct determination of k_{off} and K_d from a single experiment.[6−12] Other proven applications of NECEEM include (i) affinity analyses of proteins,[11−13] (ii) determination of temperature inside the capillary,[14] (iii) studying thermochemistry of protein−ligand interaction,[15] and (iv) selecting binding ligands from combinatorial libraries.[16−18]

SweepCE was introduced as the only non-stopped-flow method of directly finding k_{on} of protein−ligand interaction.[19] In the first work, we used nonlinear regression to fit electropherograms and find k_{on}. Although significantly simplified through explicitly solving differential equations for concentrations of A, B, and C, application of SweepCE is still limited to researchers who are familiar with mathematical modeling.

The aim of the present work was 2-fold: (i) to design a KCE method capable of directly measuring both k_{on} and k_{off} and (ii) to develop a simple mathematical approach for calculating the rate constants without nonlinear regression analysis. Both goals were achieved. The new method is termed plug−plug kinetic capillary electrophoresis (ppKCE). Conceptually, short plugs of solutions of A and B are injected into the capillary sequentially; the component with lower mobility is injected first. When the voltage is applied, the faster moving component passes through the slower moving component, resulting in complex formation. Eventually, the electrophoretic zones of A and B are separated, and the complex starts dissociating. The resulting electropherogram is qualitatively similar to that of NECEEM: it has peaks of A, B, and C and "smears" of A and B dissociated from C. However, since ppKCE does not start with the equilibrium mixture of A and B, the resulting electropherogram does not have a "memory" of K_d but, rather, has a memory of k_{on} and k_{off}. Both k_{on} and k_{off} can, thus, be calculated from a single ppKCE electropherogram using areas of peaks and smears and migration times of peaks. The mathematical analysis uses three simplifying assumptions for reaction 1. First, we assume a simple 1:1 stoichiometry of interaction between A and B; for higher-order stoichiometries, numerical modeling of KCE data has to be used. Second, we assume that only the forward reaction occurs when the zone of B moves through that of A. Finally, we assume that only the reverse process in reaction 1 occurs after the zones of A and B are separated. In this work, the ppKCE method was used to calculate k_{on} and k_{off} for interaction between a single-stranded DNA-binding protein and DNA. The new method is simple, fast, and informative. It does not require expertise in mathematical modeling and, thus, can be used by a broad community of researchers.

EXPERIMENTAL SECTION

Chemicals and Materials. Single-stranded DNA binding protein (SSB) from *Escherichia coli* and buffer components were from Sigma-Aldrich (Oakville, ON). A fluorescently labeled 15-mer DNA nucleotide (fluorescein−5′-GCGGAGCGTGGCAGG-3′) was a gift of Dr. Y. Li (McMaster University, Canada). Fused-silica capillaries were purchased from Polymicro (Phoenix, AZ). All aqueous solutions were made using the Milli-Q quality deionized water and filtered through a 0.22-μm filter (Millipore, Nepean, ON).

Instrumentation. All CE procedures were performed using the following instrumentation and common settings and operations unless otherwise stated. CE was carried out with a P/ACE MDQ apparatus (Beckman Coulter, Mississauga, ON) equipped with a fluorescence detector; a 488-nm line of an Ar-ion laser was utilized to excite fluorescence. A 50-cm-long (40 cm to a detection window) uncoated, fused-silica capillary with an inner diameter of 75 μm and outer diameter of 360 μm was used.

The sample buffers and the electrophoresis run buffer were identical: 25 mM sodium tetraborate at pH 9.3. The capillary was rinsed with the run buffer for 2 min prior to each run. Electrophoresis was carried out for a total of 10 min by an electric field of 600 V/cm with a positive electrode at the injection end of the capillary; the direction of the electroosmotic flow was from the inlet to the outlet reservoir. The temperature of the capillary was maintained at 15 ± 0.1 °C. At the end of each run, the capillary was rinsed with 0.1 M NaOH for 2 min, followed by a rinse with deionized water for 2 min.

Plug−Plug KCE. The inlet and outlet reservoirs contained the run buffer, and the capillary was prefilled with the run buffer. Injections were carried out by voltage so that plug lengths depended on both the velocity of the electroosmotic flow (common for all species) and electrophoretic velocities of injected species First, a plug of the DNA solution was injected into the capillary by a voltage pulse of 6 s × 10 kV. The length and volume of the plug were 2 mm and 8 nL, respectively. Second, to prevent the premixing caused by the differential electrophoretic mobility of DNA and SSB, we injected a short plug of the bare run buffer.

(6) Berezovski, M.; Krylov, S. N. *J. Am. Chem. Soc.* **2002**, *124*, 13674−13675.
(7) Krylov, S. N.; Berezovski, M. *Analyst* **2003**, *128*, 571−575
(8) Okhonin, V.; Krylova, S. M.; Krylov, S. N. *Anal. Chem.* **2004**, *76*, 1507−1512.
(9) Yang, P.; Whelan, R. J.; Jameson, E. E.; Kurzer, J. H.; Argetsinger, L. S.; Carter-Su, C.; Kabir, A.; Malik, A.; Kennedy, R. T. *Anal. Chem.* **2005**, *77*, 2482−2489.
(10) Drabovich, A.; Berezovski, M.; Krylov, S. N. *J. Am. Chem. Soc.* **2005**, *127*, 11224−11225.
(11) Berezovski, M.; Nutiu, R.; Li, Y.; Krylov, S. N. *Anal. Chem.* **2003**, *75*, 1382−1386.
(12) Huang, C. C.; Cao, Z.; Chang, H.-T.; Tan, W. *Anal. Chem.* **2004**, *76*, 6973−6981.
(13) Berezovski, M.; Krylov, S. N. *J. Am. Chem. Soc.* **2003**, *125*, 13451−13454.
(14) Berezovski, M.; Krylov, S. N. *Anal. Chem.* **2004**, *76*, 7114−7117.
(15) Berezovski, M.; Krylov, S. N. *Anal. Chem.* **2005**, *77*, 1526−1523.
(16) Berezovski, M.; Drabovich, A.; Krylova, S. M.; Musheev, M.; Okhonin, V.; Petrov, A.; Krylov, S. N. *J. Am. Chem. Soc.* **2005**, *127*, 3165−3171.
(17) Mendonsa, S. D.; Bowser, M. T. *J. Am. Chem. Soc.* **2004**, *126*, 20−21.
(18) Drabovich, A. P.; Berezovski, M.; Okhonin, V.; Krylov, S. N. *Anal. Chem.* **2006**, *78*, 3171−3178.
(19) Okhonin, V.; Berezovski, M.; Krylov, S. N. *J. Am. Chem. Soc.* **2004**, *126*, 7166−7167.

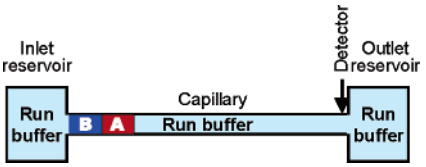

Figure 1. Schematic representation of initial and boundary conditions in ppKCE.

The injection was carried out by a voltage pulse of 8 s × 10 kV. Third, a plug of the SSB solution was injected into the capillary by a voltage pulse of 3 s × 10 kV. The length and volume of the plug were 3 mm and 12 nL, respectively. The differences in plug lengths are caused by the differences in electrophoretic mobilities of SSB and DNA. The ends of the capillary were inserted into the inlet and outlet reservoirs, and the electric field was applied to run electrophoresis. Areas of electrophoretic peaks were divided by migration times of corresponding species to ensure that areas are proportional to the amounts of the species. The areas were also normalized using fluorescein as an internal standard, to compensate for variations in volumes of injection plugs.

Determination of k_{on} and k_{off}. The k_{on} and k_{off} values were determined by inputting experimentally measured parameters into the Microsoft Excel software program, which uses the formulas provided in the result section of the paper.

RESULTS AND DISCUSSION

KCE Methods. We define KCE as CE separation of species that interact during electrophoresis. According to this definition, KCE involves two major processes: affinity interaction of A and B, described by eq 1; and separation of A, B, and C based on differences in their velocities in electrophoresis, v_A, v_B, and v_C. The two processes are described by the following general system of partial differential equations,

$$\begin{aligned}
\frac{\partial A(t,x)}{\partial t} + v_A\frac{\partial A(t,x)}{\partial x} &= -k_{on}A(t,x)\,B(t,x) + k_{off}C(t,x)\\
\frac{\partial B(t,x)}{\partial t} + v_B\frac{\partial B(t,x)}{\partial x} &= -k_{on}A(t,x)\,B(t,x) + k_{off}C(t,x)\\
\frac{\partial C(t,x)}{\partial t} + v_C\frac{\partial C(t,x)}{\partial x} &= -k_{off}C(t,x) + k_{on}A(t,x)\,B(t,x)
\end{aligned} \qquad (2)$$

where A, B, and C are concentrations of A, B, and C, respectively; t is time passed since the beginning of separation; and x is the distance from the injection end of the capillary.

The solution of system 2 depends on the initial and boundary conditions: initial distribution of A, B, and C along the capillary and the way all three components are introduced into the capillary and removed from the capillary during separation. Every set of qualitatively unique initial and boundary conditions for system 2 can define a unique KCE method.

Plug−Plug KCE. We define ppKCE as the method in which A and B are introduced into a capillary as a sequence of two short plugs when the capillary is prefilled with the run buffer and both inlet and outlet reservoirs also contain the run buffer (Figure 1). A slower moving component is injected first. In this work, we assume that A is slower than B. A spacer plug of a bare buffer can be introduced between the plugs A and B to prevent mixing of A and B and the start of reaction 1 before the beginning of electrophoresis. The initial conditions ($t = 0$) and boundary conditions ($x = 0$) for ppKCE can be formalized in the following way,

$$\begin{aligned}
&A(0,x) = [\mathrm{A}]\;\theta(x - l_A)\;\theta(l_B + l_A - x) \quad A(t,0) = 0\\
&B(0,x) = [\mathrm{B}]\;\theta(x)\;\theta(l_B - x) \quad B(t,0) = 0\\
&C(0,x) = 0 \quad C(t,0) = 0
\end{aligned} \qquad (3)$$

where [A] and [B] are concentrations of A and B, respectively, in the solutions from which the plugs are injected, l_A and l_B are lengths of the corresponding injected plugs, and $\theta(x)$ is a function which is equal to 1 when $x > 0$ and is equal to 0 when $x \le 0$.

Numerical Simulation of ppKCE. To demonstrate qualitative features of ppKCE, we simulated $A(t, x)$, $B(t, x)$, and $C(t, x)$ numerically for a fixed x. These dependencies could be used to build simulated ppKCE electropherograms, which represent a superposition of $A(t)$, $B(t)$, and $C(t)$ for x that is equal to the distance from the capillary inlet ($x = 0$) to the detector. Numerical simulation of electrophoresis, in general, is challenging because of the incompatibility of a single "space" grid with different velocities of separated species. Conventional algorithms for numerical simulation of electrophoresis use a single space grid, $x = n\Delta x$, where Δx is the length of the x increment and n is an integer representing the point number in calculations. The grid is usually based on the velocity, v, of one of the separated species: $x = \Delta x + v\Delta t$, where Δt is the time increment. Migration of species, which move with velocities different from v, is simulated "out of the grid". The out of the grid calculation leads to rounding errors that are severely aggravated in the areas of sharp fronts of electrophoretic peaks.[20] To overcome the "sharp-front" problem in simulating ppKCE electropherograms, we designed a multigrid algorithm, which solves system 2 using individual increments Δx for A, B, and C: $\Delta x_A = v_A\Delta t$, $\Delta x_B = v_B\Delta t$, and $\Delta x_C = v_C\Delta t$, respectively. On the basis of the multigrid algorithm, we wrote a computer program that calculated $A(t,x)$, $B(t,x)$, and $C(t,x)$.[20]

Figure 2 shows simulated electropherograms (dependencies of $A(t)$, $B(t)$, and $C(t)$) for different k_{off}'s and k_{on}'s. Please note the difference in scales of the y-axes in Figure 2. Figure 2a demonstrates the influence of k_{off} on electropherograms for a constant k_{on}. Since k_{on} is constant, the amount of C formed by the time when the zones of A and B are separated does not change with changing k_{off}. The variation in k_{off} changes only the rate at which C dissociates after the zones of A and B are separated. Accordingly, increasing k_{off} leads to decreasing heights of the peak of $C(t)$ and increasing areas of the smears of $A(t)$ and $B(t)$. Figure 2b illustrates the influence of k_{on} on ppKCE electropherograms for a constant k_{off}. Increasing k_{on} results in an increasing amount of C formed, leading to decreasing peaks of $A(t)$ and $B(t)$ and a growing peak of $C(t)$.

Electropherograms in ppKCE are qualitatively similar to those in NECEEM. The difference between NECEEM and ppKCE is

(20) Petrov, A.; Okhonin, V.; Berezovski, M.; Krylov, S. N. *J. Am. Chem. Soc.* **2005**, *127*, 17104−17110.

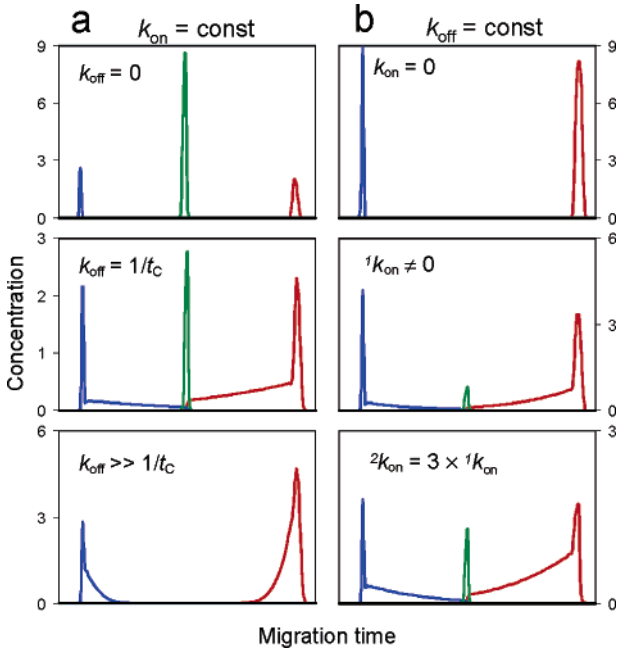

Figure 2. Simulated ppKCE electropherograms for constant k_{on} and three different k_{off}'s (panel a) and for constant k_{off} and three different k_{on}'s (panel b). Red, green, and blue colors correspond to $A(t)$, $C(t)$, and $B(t)$, respectively.

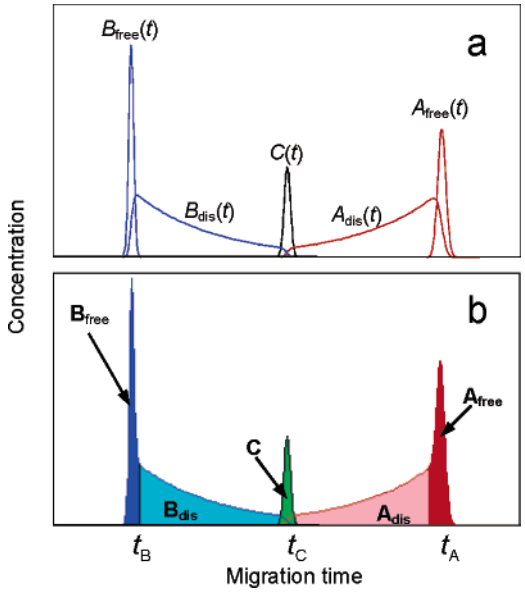

Figure 3. Panel a shows simulated ppKCE concentration profiles, with functions $A(t)$ and $B(t)$ being presented as a superposition of free and dissociated components (see equation 4). Panel b illustrates measurable parameters (areas of peaks and smears and migration times of A, B, and C), which are used for the determination of k_{on} and k_{off} without nonlinear regression analysis.

in the amount of C. NECEEM uses the equilibrium mixture of A and B, which has the highest possible amount of C for given concentrations of A and B. To measure k_{on}, ppKCE has to be performed so that quasiequilibrium is not reached during the passage of the zone of B through the zone of A. As a result, the amount of C in ppKCE is lower than that in NECEEM. As was previously demonstrated for NECEEM,[8] $A(t)$ and $B(t)$ consist of two parts (Figure 3a),

$$A(t) = A_{free}(t) + A_{dis}(t)$$
$$B(t) = B_{free}(t) + B_{dis}(t) \quad (4)$$

$A_{free}(t)$ and $B_{free}(t)$ correspond, respectively, to A and B which do not form the complex during the mixing of the zones of A and B. $A_{dis}(t)$ and $B_{dis}(t)$ correspond, respectively, to A and B, which result from the dissociation of C after the zones are separated. Areas of peaks and smears in the electropherogram, A_{free}, A_{dis}, B_{free}, B_{dis}, and C, are proportional to the amounts of corresponding species (Figure 3b).

The goal of this work was to develop a means of calculating k_{on} and k_{off} using only parameters easily measurable from a ppKCE electropherogram. These parameters are A_{free}, A_{dis}, B_{free}, B_{dis}, C and migration times of A, B, and C: t_A, t_B and t_C, respectively.

Determination of Rate Constants in ppKCE. *Determination of k_{off}.* The complex dissociation process is identical in NECEEM and ppKCE; therefore, approaches developed for the calculation of k_{off} in NECEEM are applicable to ppKCE as well.[6–8] The most practical approach uses the areas and migration times (Figure 3b).

$$k_{off} = \ln\left(\frac{C + A_{dis}}{C}\right)/t_C = \ln\left(\frac{C + A_{dis}}{B}\right)/t_C \quad (5)$$

This nonnumerical approach to the determination of k_{off} requires the assumption that no rebinding of A and B occurs when the electrophoretic zones of A and B are separated.

Determination of k_{on}. Determination of k_{on} in ppKCE without nonlinear regression analysis requires the development of a new mathematical approach. This section is devoted to introducing such an approach; mathematical details can be found in the Supporting Information. When the zone of B passes through the zone of A, the forward reaction 1 (the formation of C) occurs. We make a simplifying assumption that the reverse reaction 1 (the dissociation of C) is negligible during this time. The time required for zone B to pass through zone A is determined as $t_{pass} = (l_A + l_B)/|v_A - v_B|$. For the assumption to be satisfied, this time should be much shorter than the characteristic time of complex dissociation $t_{char} = 1/k_{off}$. This condition is typically satisfied for complexes between biological polymers, for which k_{off} values are on the order of 10^{-3} s^{-1} or even smaller, whereas t_{pass} can be as short as 1 s. If the assumption of negligible dissociation is satisfied, the exact solution of eq 2 for $A(t, x)$ and $B(t, x)$ is the following:

$$A(t,x) = \frac{\partial\lambda(t,x)}{\partial t} + v_B\frac{\partial\lambda(t,x)}{\partial x}$$
$$B(t,x) = \frac{\partial\lambda(t,x)}{\partial t} + v_A\frac{\partial\lambda(t,x)}{\partial x} \quad (6)$$
$$\lambda = \frac{1}{k_{on}}\ln\{\alpha(x - tv_B) + \beta(x - tv_A)\}$$

The correctness of this solution can be confirmed by direct substitution of solution 6 into system 2. Initial concentrations of

A and B can be expressed as

$$A(0,x) = \frac{(v_B - v_A)\ d\beta(x)/dx}{k_{on}(\alpha(x) + \beta(x))}$$
$$B(0,x) = \frac{(v_A - v_B)\ d\alpha(x)/dx}{k_{on}(\alpha(x) + \beta(x))} \quad (7)$$

We assume that the initial concentration profiles of A and B do not overlap prior to the beginning of separation. In such a case, the solution of system 7 for functions α and β can be found.

$$\alpha(x) = \exp\{k_{on}\int_{-\infty}^{x} B(0,y)\ dy/(v_A - v_B)\} - \beta(-\infty)$$
$$\beta(x) = \exp\{k_{on}\int_{-\infty}^{x} B(0,y)\ dy/(v_A - v_B)\} \times (\exp\{k_{on}\int_{-\infty}^{x} A(0,y)\ dy/(v_B - v_A)\} - 1) + \beta(-\infty) \quad (8)$$

From solution 8, using 6, we can obtain the solution for $A(t, x)$, which describes the distribution of component A along the capillary at any given time.

$$A(t,x) = \frac{(v_B - v_A)\dfrac{\partial\beta(x - tv_A)}{\partial x}}{k_{on}(\beta(x - tv_A) + \alpha(x - tv_B))} = -\frac{(v_B - v_A)}{k_{on}v_A} \times \frac{\partial}{\partial t}\ln\{\exp\{k_{on}\int_{-\infty}^{\infty} B(0,y)dy/(v_A - v_B)\} \times (\exp\{k_{on}\int_{-\infty}^{x - v_A t} A(0,y)\ dy/(v_B - v_A)\} - 1) + 1\} \quad (9)$$

The solution for $B(t, x)$ can be found in a similar way; however, due to the mass balance we do not need $B(t, x)$ to calculate k_{on}. We further define A_{in} and B_{in} as total amounts of A and B, respectively, in the capillary before mixing the zones; A_{out} is defined as the amount of A remaining free when the zones of A and B are separated (B_{out} is not needed because of the mass balance).

$$A_{in} = S\int_{-\infty}^{\infty} A(0,x)\ dx$$
$$B_{in} = S\int_{-\infty}^{\infty} B(0,x)\ dx \quad (10)$$
$$A_{out} = v_A S\int_{-\infty}^{\infty} A(t,x)\ dt$$

where S is the area of the capillary cross section. These three parameters are linked with peak areas in a ppKCE electropherogram with the precision of a conversion constant, b (Figure 3b).

$$A_{in} = b(A_{free} + A_{dis} + C)$$
$$B_{in} = b(B_{free} + B_{dis} + C) \quad (11)$$
$$A_{out} = bA_{free}$$

A_{in} and B_{in} can be also defined through concentrations of A ([A]) and B ([B]) in the solution they are injected from, as well as by plug lengths and capillary cross section.

$$A_{in} = [A]l_A S$$
$$B_{in} = [B]l_B S \quad (12)$$

By combining expressions 9 and 10, we can obtain the following expression for A_{out}.

$$A_{out} = \frac{S(v_B - v_A)}{k_{on}} \times \ln(\exp(k_{on}A_{in}/(S(vB - vA))) - 1) \times \exp(k_{on}B_{in}/(S(vA - vB))) + 1 \quad (13)$$

To simplify eq 13, we introduce the following parameter:

$$\epsilon = k_{on}A_{in}/(S(v_B - v_A)) \quad (14)$$

By using 14, eq 13 can be expressed as:

$$A_{out}/A_{in} = \frac{1}{\epsilon}\ln\ (\exp(\epsilon) - 1) \times (\exp(-\epsilon(B_{in}/A_{in})) + 1) \quad (15)$$

Ratios A_{out}/A_{in} and B_{in}/A_{in} in eq 15 can be expressed through controlled and experimentally determined parameters,

$$A_{out}/A_{in} = A_{free}/(A_{free} + A_{dis} + C)$$
$$B_{in}/A_{in} = [B]l_B/([A]l_A) \quad (16)$$

where [B] and [A] are concentration of B and A injected into the capillary. By using 16, eq 15 can then be converted into

$$A_{free}/(A_{free} + A_{dis} + C) = 1/\epsilon \times \ln\{(\exp(\epsilon) - 1)\exp(-\epsilon \times ([B]l_B/([A]l_A))) + 1\} \quad (17)$$

In this equation, all parameters but ϵ are either controlled or measurable. The value of ϵ can be determined from eq 17 using the Microsoft Excel program as described in the appendix.

Finally, using ϵ calculated from 17, the value of k_{on} can be calculated from the rearranged eq 14 in which A_{in} was substituted with $[A]l_A S$ (see eq 12).

$$k_{on} = \epsilon(v_B - v_A)/([A]l_A) \quad (18)$$

The velocities in eq 18 can be replaced by the effective capillary length, L, divided by corresponding migration times (t_B or t_A).

$$k_{on} = \epsilon L(1/t_B - 1/t_A)/([A]l_A) \quad (19)$$

This allows determination of k_{on} when A_{free}, A_{dis}, C, t_B, and t_A are determined from a ppKCE electropherogram. The other four parameters, [B], [A], l_B, and l_A, are controlled by an experimentalist.

Assumptions. Table 1 can be used to identify a range of experimental conditions that satisfy the assumptions of the model.

Table 1. Upper Limits for k_{off} Values as a Function of Concentrations, Time of Electrophoretic Zones Passing through Each Other (t_{pass}), and k_{on} Values

		max (A, B) (M)					
k_{on} (M^{-1} s^{-1})	t_{pass} (s)	10^{-4}	10^{-5}	10^{-6}	10^{-7}	10^{-8}	10^{-9}–10^{-12}
10^3	1	1.00×10^{0}	1.00×10^{0}	1.00×10^{0}	1.00×10^{0}	1.00×10^{0}	1.00×10^{0}
	10	1.00×10^{-1}	1.00×10^{-1}	1.00×10^{-1}	1.00×10^{-1}	1.00×10^{-1}	1.00×10^{-1}
	40	1.25×10^{-2}	2.50×10^{-2}	2.50×10^{-2}	2.50×10^{-2}	2.50×10^{-2}	2.50×10^{-2}
	80	3.13×10^{-3}	1.25×10^{-2}	1.25×10^{-2}	1.25×10^{-2}	1.25×10^{-2}	1.25×10^{-2}
10^4	1	1.00×10^{0}	1.00×10^{0}	1.00×10^{0}	1.00×10^{0}	1.00×10^{0}	1.00×10^{0}
	10	2.00×10^{-2}	1.00×10^{-1}	1.00×10^{-1}	1.00×10^{-1}	1.00×10^{-1}	1.00×10^{-1}
	40	1.25×10^{-3}	1.25×10^{-2}	2.50×10^{-2}	2.50×10^{-2}	2.50×10^{-2}	2.50×10^{-2}
	80	3.13×10^{-4}	3.13×10^{-3}	1.25×10^{-2}	1.25×10^{-2}	1.25×10^{-2}	1.25×10^{-2}
10^5	1	2.00×10^{-1}	1.00×10^{0}	1.00×10^{0}	1.00×10^{0}	1.00×10^{0}	1.00×10^{0}
	10	2.00×10^{-3}	2.00×10^{-2}	1.00×10^{-1}	1.00×10^{-1}	1.00×10^{-1}	1.00×10^{-1}
	40	1.30×10^{-4}	1.25×10^{-3}	1.25×10^{-2}	2.50×10^{-2}	2.50×10^{-2}	2.50×10^{-2}
	80	3.13×10^{-5}	3.13×10^{-4}	3.13×10^{-3}	1.25×10^{-2}	1.25×10^{-2}	1.25×10^{-2}
10^6	1	2.00×10^{-2}	2.00×10^{-1}	1.00×10^{0}	1.00×10^{0}	1.00×10^{0}	1.00×10^{0}
	10	2.00×10^{-4}	2.00×10^{-3}	2.00×10^{-2}	1.00×10^{-1}	1.00×10^{-1}	1.00×10^{-1}
	40	1.30×10^{-5}	1.30×10^{-4}	1.25×10^{-3}	1.25×10^{-2}	2.50×10^{-2}	2.50×10^{-2}
	80	3.13×10^{-6}	3.13×10^{-5}	3.13×10^{-4}	3.13×10^{-3}	1.25×10^{-2}	1.25×10^{-2}
10^7	1	2.00×10^{-3}	2.00×10^{-2}	2.00×10^{-1}	1.00×10^{0}	1.00×10^{0}	1.00×10^{0}
	10	2.00×10^{-5}	2.00×10^{-4}	2.00×10^{-3}	2.00×10^{-2}	1.00×10^{-1}	1.00×10^{-1}
	40	1.30×10^{-6}	1.30×10^{-5}	1.30×10^{-4}	1.25×10^{-3}	1.25×10^{-2}	2.50×10^{-2}
	80	3.13×10^{-7}	3.13×10^{-6}	3.13×10^{-5}	3.13×10^{-4}	3.13×10^{-3}	1.25×10^{-2}

Table 1 lists upper suitable limits for k_{off} as a function of k_{on}, time of zones of A and B passing through each other (t_{pass}), and the highest of the concentrations of A and B (max (A, B)). The limits for k_{off} values were determined using formula 39 in the Supporting Information. To test whether the experimental conditions are acceptable for the model, the user has to choose the column with the concentration closest to the highest of the two concentrations ([A] and [B]) used in experiment; then choose the row with the k_{on} value closest to the anticipated k_{on} value; and finally, choose the subrow with t_{pass} which correspond to the given experimental conditions. The corresponding value inside the double-border portion of the table would give the upper acceptable limit of the k_{off} value for the mathematical model to work. If the dissociation is faster than the found upper limit of acceptable k_{off}, one should choose more appropriate conditions to satisfy the assumptions. First, a separation buffer can be found, which facilitates a greater differential velocity of A and B and, thus, a shorter t_{pass}. Second, the initial concentrations of A and B can be decreased. Finally, the lengths of the plugs of A and B can be decreased. We anticipate that suitable conditions will be found for most types of biomolecular interactions.

The conditions found from Table 1 to satisfy the assumptions for the model also guarantee that equilibrium is not reached. In addition, the fact that equilibrium is not reached can be confirmed by comparing NECEEM and ppKCE data. If the C/A_{free} ratio is smaller for ppKCE than that for NECEEM, then the equilibrium is not reached (the maximum ratio is achieved at equilibrium).

Application of ppKCE to Protein–Ligand Complexes. To demonstrate the practical application of the method, we used interaction between a single-stranded DNA binding protein (SSB) and ssDNA. DNA was fluorescently labeled to facilitate sensitive detection. SSB did not have a fluorophore and was not detectable; the complex of SSB with fluorescently labeled DNA was detectable. Under the separation conditions that were chosen,

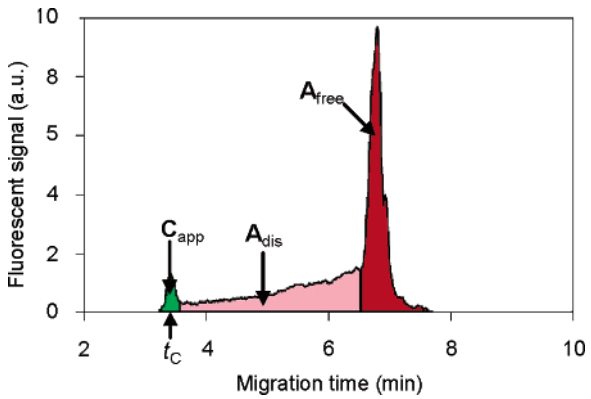

Figure 4. Experimental electropherogram for 200 nM SSB with 200 nM fluorescently labeled DNA interaction using ppKCE method. The areas used in analysis are color-coded: green for the complex, pink for the decay, and red for the unreacted DNA.

DNA was migrating slower than SSB, so we will be referring to DNA and SSB as A and B components, respectively, to be consistent with the previous theoretical consideration. An experimental ppKCE electropherogram for the SSB–DNA interaction is shown in Figure 4. All experimental values presented below without deviations correspond to the data in this figure. To determine the left boundary of the peak of A_{free}, the ppKCE electropherogram was compared with a control electropherogram with DNA only. The boundary between C and A_{dis} can be accurately determined using fluorescence anisotropy as we described earlier.[21] Relative deviations of peak areas associated with uncertainties of the boundaries are typically within 10%. The values of A_{dis} and A_{free}, the apparent value of C (C_{app}), and the migration time of C and A were obtained from the electropherogram: $A_{dis} = 121$, $A_{free} = 128$, $C_{app} = 15.9$, and $t_C = 204$ s. C_{app} differs from C by a relative fluorescence quantum yield, q, of C with respect to that of free A: $C_{app} = C \times q$. The value of q

(21) Krylov, S. N.; Berezovski, M. *Analyst* **2003**, *128*, 571–575.

was calculated by measuring the total areas in two electropherograms. The first was obtained from A in the presence of B (Figure 4), and the second was in the absence of B (not shown). The total area in the absence of B was $A = 294$. The total areas in the 2 electropherograms should be identical if C_{app} is divided by q.

$$A = C_{app}/q + A_{dis} + A_{free} \quad (20)$$

From this equation we can find q.

$$q = C_{app}/(A - A_{dis} - A_{free}) \quad (21)$$

The relative quantum yield calculated from eq 21 was $q = 0.35$. This allowed us to obtain $C = C_{app}/q = 45$. This value along with the above values for A_{dis}, A_{free}, and t_C were used in the following calculation of the rate constants. For simplicity, we assumed that only one effective k_{on} and k_{off} constants exist.

The average k_{off} value and its experimental deviation, $k_{off} = (6.4 \pm 0.8) \times 10^{-3}$ s^{-1}, were calculated using eq 5 from five consecutive experiments similar to the one depicted in Figure 4.

To determine k_{on}, we used the same values of A_{dis}, A_{free}, and C, as well as [A] $= 2.0 \times 10^{-7}$ M, [B] $= 2.0 \times 10^{-7}$ M, $l_A = 0.40$ cm, $l_B = 0.40$ cm, $t_A = 400$ s, $t_B = 138$ s, and $L = 40$ cm. The value of ϵ was calculated from expression 17 using the "Goal Seek" procedure in Excel (see the appendix). For the electropherogram depicted in Figure 4, the value of ϵ was equal to 1.23.

The average k_{on} value and its experimental deviation, $k_{on} = (2.9 \pm 0.8) \times 10^6$ M^{-1} s^{-1}, were determined using eq 19 from the same five experiments, which were used for the calculation of k_{off}.

The values of k_{off} and k_{on} determined by ppKCE were in good agreement with those obtained by other KCE methods.[6,7,19,20] The previously reported k_{off} is slightly higher because CE separations in the earlier works were performed at higher temperatures using CE instrumentation with no temperature control. It is instructive to compare our data on SSB−DNA binding with those published by others. LeCaptain et al.[22] used CE coupled with single molecule fluorescence correlation spectroscopy to measure $K_d = 2$ nM. This result is close to ours: $K_d = k_{off}/k_{on} = 6.4 \times 10^{-3}/\ 2.9 \times 10^6 = 2.2 \times 10^{-9}$ M. The data for k_{on} and k_{off} for SSB−DNA interactions are scarce, but those that are available show tremendous differences, depending on substrates and experimental conditions used. SPR data show that in the noncooperative mode of binding, SSB binds DNA with the following rate constants: $k_{off} = 1.34 \times 10^{-4}$ s^{-1} and $k_{on} = 1.1 \times 10^6$ M^{-1} s^{-1}. This result is comparable with ours in terms of k_{on}; the k_{off} obtained by SPR is lower most likely due to the low pH.[23] The stopped-flow measurements on long DNA revealed the k_{on} value of 2.1×10^8 M^{-1} s^{-1}, which differs by 2 orders of magnitude from SPR and ppKCE data. This difference is most likely due to the fact that SSB exhibits highly cooperative binding for long DNA substrates.[24] Kozlov and Lohman reported that, depending on the substrate and experimental conditions, k_{on} for SSB−DNA interaction can vary between 10^3 and 10^8 M^{-1} s^{-1}.[25] Our own data and the results by others indicate that the kinetic parameters of protein−DNA interactions are so sensitive to conditions that it is imperative that the rate constants be measured de novo when experimental conditions change. This emphasizes the need for simple, reliable, sensitive, and fast methods for kinetic studies of protein−DNA interactions. The methods of KCE augment the arsenal of tools available for such studies.

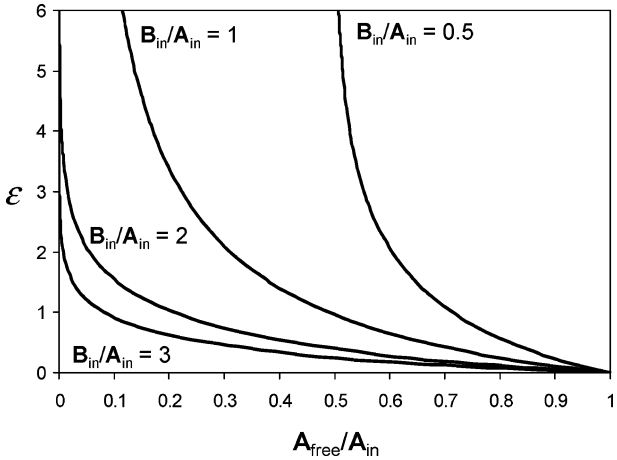

Figure 5. Example of diagrams that can serve for rapid determination of ϵ.

CONCLUSIONS

In this work, we developed a novel KCE method for direct determination of rate constants of complex formation and dissociation from one experimental electropherogram. In addition, we developed a simple mathematical approach for calculating the rate constants without performing nonlinear regression analysis so that the method does not require expertise in mathematical modeling. So far, there has not been a method that allowed direct measurement of both rate constants. The method presented is simple and robust. It requires only nanoliter volumes of reagents and can be readily adjusted for different ranges of both constants. We believe that this method will be useful for screening large libraries for drug candidates as well as the development of novel research and diagnostic tools. We also foresee that simple mathematics will be developed for other KCE method,[20] thus making them practical analytical tools for a large community of molecular scientists.

APPENDIX

The Use of Microsoft Excel for Calculations of k_{on} and k_{off}. It is possible to find ϵ from eq 17 by using the embedded standard procedure Goal Seek in the Tools menu of Microsoft Excel. Before calling the procedure, all experimental values required for calculations have to be entered in individual cells on an Excel spreadsheet. In addition, the initial value of ϵ for the first iteration has to be entered; $\epsilon = 1$ can be used as a default number. Another cell should contain the difference between the left-hand side and the right-hand side of eq 17. To increase the accuracy of numerical calculations, this difference can be multiplied by a large number; for example, 1000. The Goal Seek procedure can be then called.

(22) LeCaptain, D. J.; Michel, M. A.; Van Orden, A. *Analyst* **2001**, *126*, 1279−1284.
(23) Fisher, R. J.; Fivash, M.; Casas-Finet, J.; Bladen, S.; McNitt, K. L. *Methods* **1994**, *6*, 121−133.
(24) Witte, G.; Urbanke, C.; Curth, U. *Nucleic Acids Res.* **2005**, *33*, 1662−1670.
(25) Kozlov A. G.; Lohman T. M. *Biochemistry* **2002**, *41*, 11611−11627.

The parameters in the Parameter menu should be set up in the following way. The cell containing the difference between the left-hand side and right-hand side of eq 17 should be chosen for the Set Cell parameter. The To Value parameter should be set to 0. The By Changing Cell parameter should be referenced to the cell containing the initial value of ϵ. The Goal Seek function would then give the value of ϵ required for the determination of k_{on} with eq 19. An example of such an Excel spreadsheet can be found in the Research section of the following web page: www.chem.yorku.ca/profs/krylov.

For routine work, such as screening large libraries of compounds for their ability to bind a target, it is possible to construct a family of diagrams of the $A_{free}/(A_{free} + A_{dis} + C)$ dependence on ϵ at fixed B_{in}/A_{in} ratios, from which ϵ can be determined. An example of such diagrams is shown in Figure 5.

GLOSSARY

t	time passed from beginning of separation
x	distance from inlet of capillary
A, B	names of reacting components
C	noncovalent complex of A and B
$A(t, x)$	concentration of A as a function of t and x
$B(t, x)$	concentration of B as a function of t and x
$C(t,x)$	concentration of C as a function of t and x
A_{in}	total amount of A inside capillary before reacting A and B
B_{in}	total amount of B inside capillary before reacting A and B
A_{free}	total amount of nonreacted A after reacting A and B
B_{free}	total amount of nonreacted B after reacting of A and B
A_{dis}	total amount of A dissociated from C before C passed detector
B_{dis}	total amount of B dissociated from C before C passed detector
C	amount of intact C reaching detector
$A_{free}(t)$	concentration of nonreacted A as a function of t
$B_{free}(t)$	concentration of nonreacted B as a function of t
$A_{dis}(t)$	concentration (in the detection point) of A dissociated from C as a function of t
$B_{dis}(t)$	concentration (in the detection point) of B dissociated from C as a function of t
l_A	length of plug of component A
l_B	length of plug of component B
v	effective velocity in electrophoresis equal to the sum of electrophoretic and electroosmotic velocities
v_A	effective velocity of A
v_B	effective velocity of B
v_C	effective velocity of C
k_{on}	bimolecular rate constant of complex formation
k_{off}	unimolecular rate constant of complex dissociation
S	area of capillary's cross section
L	capillary length from inlet to detector
ϵ	dimensionless parameter determined from expression 17
t_{char}	characteristic time of dissociation of C; equal to $1/k_{off}$
t_{pass}	time necessary for plugs of A and B to pass through each other
t_A	migration time of A
t_B	migration time of B
t_C	migration time of C
Δt	time increment in numerical calculations
Δx	space increment in numerical calculations
Δx_A	individual space increment for A
Δx_B	individual space increment for B
Δx_C	individual space increment for C

ACKNOWLEDGMENT

This work was supported by the Natural Sciences and Engineering Research Council of Canada. The authors thank Dr. Y. Li for providing the fluorescently labeled DNA.

SUPPORTING INFORMATION AVAILABLE

Supporting mathematical appendix. This material is available free of charge via the Internet at http://pubs.acs.org.

Received for review January 15, 2006. Accepted April 19, 2006.

AC060108I

SUPPORTING INFORMATION

Plug-Plug Kinetic Capillary Electrophoresis: A Method for Direct Determination of Rate Constants of Complex Formation and Dissociation

Victor Okhonin, Alexander Petrov, Maxim Berezovski, and Sergey N. Krylov

Department of Chemistry, York University, Toronto, Ontario M3J 1P3, Canada

1. Kinetic Capillary Electrophoresis

The general mathematical model was developed for Kinetic Capillary Electrophoresis (KCE), which we define as interaction of species in capillary electrophoresis under non-equilibrium conditions. In KCE, there are two major processes: interactions between components A and B resulting in the formation of complex C and separation of A, B, and C, based on differences in electrophoretic mobilities. Those processes are described by the system of partial differential equations:

$$\begin{aligned}
&\frac{\partial A(t,x)}{\partial t} + v_{\mathrm{A}} \frac{\partial A(t,x)}{\partial x} = -k_{\mathrm{on}} A(t,x) B(t,x) + k_{\mathrm{off}} C(t,x) \\
&\frac{\partial B(t,x)}{\partial t} + v_{\mathrm{B}} \frac{\partial B(t,x)}{\partial x} = -k_{\mathrm{on}} A(t,x) B(t,x) + k_{\mathrm{off}} C(t,x) \\
&\frac{\partial C(t,x)}{\partial t} + v_{\mathrm{C}} \frac{\partial C(t,x)}{\partial x} = -k_{\mathrm{off}} C(t,x) + k_{\mathrm{on}} A(t,x) B(t,x)
\end{aligned} \tag{1}$$

Here, A, B, and C are concentrations of A, B, and C, respectively; t is time passed since the beginning of separation; x is the distance from the injection end of the capillary. The solution of system (1) depends on the initial and boundary conditions: initial distribution of A, B, and C along the capillary and the way how all three components are introduced into the capillary and removed from the capillary during separation. Every set of qualitatively unique initial and boundary conditions for system (1) can define a unique KCE method.

2. Plug-Plug Kinetic Capillary Electrophoresis

In the ppKCE method, components A and B are introduced as two separate short plugs with the capillary pre-filled with a run buffer while both inlet and outlet reservoirs contain the run buffer as well. The initial and boundary conditions can be, thus, represented as:

$$\begin{aligned}
&A(0,x) = 0, \quad x > l_{\mathrm{B}} + l_{\mathrm{A}}, \quad x < l_{\mathrm{A}}, && A(t,0) = 0, \\
&B(0,x) = 0, \quad x < l_{\mathrm{B}}, && B(t,0) = 0, \\
&C(0,x) = 0, && C(t,0) = 0
\end{aligned} \tag{2}$$

where l_{A} and l_{B} are lengths of plugs A and B, respectively.

The slower moving component A is injected first, followed by the faster moving component B. When the voltage is applied, the zone of B is passing through that of A, resulting in the formation of complex C. When the zones of A and B are separated, the C starts dissociating.

3. Determination of k_{on} in ppKCE

The k_{on} rate constant for ppKCE can be determined without nonlinear-regression analysis. To do so, the following simplifying assumptions has to be made: the complex formation reaction occurs only when the zone of B moves through that of A, while the dissociation process occurs only after the zones of A and B are separated.

Here we analyze processes, described by the following system of partial differential equations:

$$\frac{\partial A(t,x)}{\partial t} + v_A \frac{\partial A(t,x)}{\partial x} = -k_{on} A(t,x) B(t,x)$$
$$\frac{\partial B(t,x)}{\partial t} + v_B \frac{\partial B(t,x)}{\partial x} = -k_{on} A(t,x) B(t,x) \quad (3)$$

Equations (3) represent a reduced system of equations (1) which is obtained for $k_{off} = 0$. Accordingly, the terms associated with C in system (1) become equal to 0. In more details constrains in which it's possible to use (3) instead (1), discussed below, in section 4 of Supporting Information.

There is a general analytical solution of system (3). To find it we introduce two new variables:

$$\omega = x - v_A t,$$
$$\gamma = v_B t - x \quad (4)$$

Using (4), we can rewrite (3) as:

$$\frac{\partial A(\omega,\gamma)}{\partial \gamma} = -k_{on} A(\omega,\gamma) B(\omega,\gamma) / (v_B - v_A)$$
$$\frac{\partial B(\omega,\gamma)}{\partial \omega} = -k_{on} A(\omega,\gamma) B(\omega,\gamma) / (v_B - v_A) \quad (5)$$

From system (5) we can conclude that:

$$\frac{\partial A(\omega,\gamma)}{\partial \gamma} = \frac{\partial B(\omega,\gamma)}{\partial \omega} \quad (6)$$

Integration of (6) with respect to γ, between any γ_0 and γ, gives us:

$$A(\omega,\gamma) - A(\omega,\gamma_0) = \partial_\omega \int_{\gamma_0}^{\gamma} B(\omega,\gamma')d\gamma' \quad (7)$$

This expression can be rewritten as:

$$A(\omega,\gamma) = \partial_\omega \left(\int_{\gamma_0}^{\gamma} B(\omega,\gamma')d\gamma' + \int_{\omega_0}^{\omega} A(\omega',\gamma_0)d\omega' + const \right) \quad (8)$$

where ω_0 is a constant.

We then introduce function λ as:

$$\lambda(\omega,\gamma) = \int_{\gamma_0}^{\gamma} B(\omega,\gamma')d\gamma' + \int_{\omega_0}^{\omega} A(\omega',\gamma_0)d\omega' + const \quad (9)$$

Thus (8) can be presented as:

$$A(\omega,\gamma) = \partial_\omega \lambda(\omega,\gamma) \quad (10)$$

From (9) we can express function B as:

$$B(\omega,\gamma) = \partial_\gamma \lambda(\omega,\gamma) \quad (11)$$

Using equations (8) and (9) we can present system (5) in the form of one equation only:

$$\frac{\partial^2 \lambda(\omega,\gamma)}{\partial\gamma\partial\omega} = -k_{on} \frac{\partial\lambda(\omega,\gamma)}{\partial\gamma} \frac{\partial\lambda(\omega,\gamma)}{\partial\omega} / (v_B - v_A) \quad (12)$$

Equation (12) can be written as:

$$\partial^2_{\gamma\omega} \exp(-k_{on}\lambda(\omega,\gamma)/(v_B - v_A)) = 0 \quad (13)$$

To simplify (13) we introduce function Q:

$$Q(\omega,\gamma) = \exp(-k_{on}\lambda(\omega,\gamma)/(v_B - v_A)) \quad (14)$$

Using equation (14) we can rewrite (13) as:

$$\partial^2_{\gamma\omega} Q(\omega,\gamma) = 0 \quad (15)$$

The general solution of linear equation (15) can be presented in the following form:

$$Q(\omega,\gamma)=\alpha(-\gamma)+\beta(\omega) \tag{16}$$

Finally, by returning from variables ω and γ to *t* and *x*, the general analytical solution of equations (3) for $A(t,x)$ and $B(t,x)$ can be obtained:

$$\begin{aligned} A(t,x)&=\frac{\partial\lambda(t,x)}{\partial t}+v_{\mathrm{B}}\frac{\partial\lambda(t,x)}{\partial x}\\ B(t,x)&=\frac{\partial\lambda(t,x)}{\partial t}+v_{\mathrm{A}}\frac{\partial\lambda(t,x)}{\partial x} \end{aligned} \tag{17}$$

where $\lambda=\frac{1}{k_{\mathrm{on}}}\ln\left\{\alpha(x-tv_{\mathrm{B}})+\beta(x-tv_{\mathrm{A}})\right\}$

The correctness of this solution can be also confirmed by direct substitution of solution (17) into system (3). Functions α and β can be found, by using initial concentrations $A(0,x)$ and $B(0,x)$ in system (17):

$$\begin{aligned} A(0,x)&=\frac{(v_{\mathrm{B}}-v_{\mathrm{A}})d\beta(x)/dx}{k_{\mathrm{on}}\left(\alpha(x)+\beta(x)\right)}\\ B(0,x)&=\frac{(v_{\mathrm{A}}-v_{B})d\alpha(x)/dx}{k_{\mathrm{on}}\left(\alpha(x)+\beta(x)\right)} \end{aligned} \tag{18}$$

Expressions (18) can be rewritten as:

$$\begin{aligned} d\beta(x)/dx&=k_{\mathrm{on}}A(0,x)\left(\alpha(x)+\beta(x)\right)/(v_{\mathrm{B}}-v_{\mathrm{A}})\\ d\alpha(x)/dx&=k_{\mathrm{on}}B(0,x)\left(\alpha(x)+\beta(x)\right)/(v_{\mathrm{A}}-v_{B}) \end{aligned} \tag{19}$$

From (19) the sum of α and β can be expressed as:

$$\alpha(x)+\beta(x)=(\alpha(-\infty)+\beta(-\infty))\exp\left\{k_{\mathrm{on}}\int_{-\infty}^{x}\left(A(0,y)-B(0,y)\right)dy/(v_{\mathrm{B}}-v_{\mathrm{A}})\right\} \tag{20}$$

From equation (18) we can conclude that by multiplying α and β by any constant value except zero wouldn't change the system of equations. Thus, we are free to choose any value for:

$$\alpha(-\infty)+\beta(-\infty) \tag{21}$$

For the simplicity, lets assume that:

$$\alpha(-\infty)+\beta(-\infty)=1 \tag{22}$$

From (19), (20), and (22) we can get the following two equations:

$$\begin{aligned} d\beta(x)/dx&=k_{\mathrm{on}}A(0,x)\exp\left\{k_{\mathrm{on}}\int_{-\infty}^{x}\left(A(0,y)-B(0,y)\right)dy/(v_{\mathrm{B}}-v_{\mathrm{A}})\right\}/(v_{\mathrm{B}}-v_{\mathrm{A}})\\ d\alpha(x)/dx&=k_{\mathrm{on}}B(0,x)\exp\left\{k_{\mathrm{on}}\int_{-\infty}^{x}\left(A(0,y)-B(0,y)\right)dy/(v_{\mathrm{B}}-v_{\mathrm{A}})\right\}/(v_{\mathrm{A}}-v_{B}) \end{aligned} \tag{23}$$

From system (23) the solutions for α and β are:

$$\begin{aligned} \beta(x)&=\beta(-\infty)+k_{\mathrm{on}}\int_{0}^{x}A(0,x')\exp\left\{k_{\mathrm{on}}\int_{-\infty}^{x'}\left(A(0,y)-B(0,y)\right)dy/(v_{\mathrm{B}}-v_{\mathrm{A}})\right\}dx'/(v_{\mathrm{B}}-v_{\mathrm{A}})\\ \alpha(x)&=1-\beta(-\infty)+k_{\mathrm{on}}\int_{0}^{x}B(0,x')\exp\left\{k_{\mathrm{on}}\int_{-\infty}^{x'}\left(A(0,y)-B(0,y)\right)dy/(v_{\mathrm{B}}-v_{\mathrm{A}})\right\}dx'/(v_{\mathrm{A}}-v_{\mathrm{B}}) \end{aligned} \tag{24}$$

Generally, a system of equations similar to (24) cannot be simplified. But in our case, if initial concentration profiles of A and B do not overlap prior to the beginning of separation, we can simplify system (24) to the following:

$$\beta(x) = \beta(-\infty) + k_{on} \exp\left\{k_{on} \int_{-\infty}^{\infty} B(0,y)dy/(v_A - v_B)\right\} \times$$

$$\times \int_{-\infty}^{x} A(0,x') \exp\left\{k_{on} \int_{-\infty}^{x'} A(0,y)dy/(v_B - v_A)\right\} dx'/(v_B - v_A) \tag{25}$$

$$\alpha(x) = 1 - \beta(-\infty) + \int_{-\infty}^{x} B(0,x') \exp\left\{k_{on} \int_{-\infty}^{x'} B(0,y)dy/(v_A - v_B)\right\} dx'/(v_A - v_B)$$

From (25) the solutions for α and β are:

$$\begin{aligned} \beta(x) &= \beta(-\infty) + \exp\left\{k_{on} \int_{-\infty}^{\infty} B(0,y)dy/(v_A - v_B)\right\} \left(\exp\left\{k_{on} \int_{-\infty}^{x} A(0,y)dy/(v_B - v_A)\right\} - 1\right) \\ \alpha(x) &= \exp\left\{k_{on} \int_{-\infty}^{x} B(0,y)dy/(v_A - v_B)\right\} - \beta(-\infty) \end{aligned} \tag{26}$$

From solutions (26), by using initial conditions from (18), we can obtain the solution for $A(t,x)$, which describes the distribution of component A along capillary at any given time:

$$A(t,x) = \frac{(v_B - v_A)\partial_x \beta(x - tv_A)}{k_{on}\left(\beta(x - tv_A) + \alpha(x - tv_B)\right)} =$$

$$= \frac{(v_B - v_A)}{k_{on}} \times \frac{\partial_x \left[\exp\left\{k_{on} \int_{-\infty}^{x - v_A t} B(0,y)dy/(v_A - v_B)\right\} \times \left(\exp\left\{k_{on} \int_{-\infty}^{x - v_A t} A(0,y)dy/(v_B - v_A)\right\} - 1\right)\right]}{\exp\left\{k_{on} \int_{-\infty}^{x - v_A t} B(0,y)dy/(v_A - v_B)\right\} \times \left(\exp\left\{k_{on} \int_{-\infty}^{x - v_A t} A(0,y)dy/(v_B - v_A)\right\} - 1\right) + } =$$

$$+ \exp\left\{k_{on} \int_{-\infty}^{x - tv_B} B(0,y)dy/(v_A - v_B)\right\}$$

$$= \frac{(v_B - v_A)}{k_{on}} \times \frac{\partial_x \left[\exp\left\{k_{on} \int_{-\infty}^{\infty} B(0,y)dy/(v_A - v_B)\right\} \times \left(\exp\left\{k_{on} \int_{-\infty}^{x - v_A t} A(0,y)dy/(v_B - v_A)\right\} - 1\right)\right]}{\exp\left\{k_{on} \int_{-\infty}^{\infty} B(0,y)dy/(v_A - v_B)\right\} \times \left(\exp\left\{k_{on} \int_{-\infty}^{x - v_A t} A(0,y)dy/(v_B - v_A)\right\} - 1\right) + 1} =$$

$$= -\frac{(v_B - v_A)}{k_{on} v_A} \partial_t \ln\left\{\exp\left\{k_{on} \int_{-\infty}^{\infty} B(0,y)dy/(v_A - v_B)\right\} \times \left(\exp\left\{k_{on} \int_{-\infty}^{x - v_A t} A(0,y)dy/(v_B - v_A)\right\} - 1\right) + 1\right\} \tag{27}$$

To determine k_{on}, we define parameters $\mathbf{A}_{in}$ and $\mathbf{B}_{in}$ as total initial amounts of A and B, respectively, in the capillary before mixing; $\mathbf{A}_{free}$ is defined as the total amount of non-reacted A after the zones of A and B are separated:

$$\begin{aligned} \mathbf{A}_{in} &= S \int_{-\infty}^{\infty} A(0,x)dx \\ \mathbf{B}_{in} &= S \int_{-\infty}^{\infty} B(0,x)dx \\ \mathbf{A}_{free} &= v_A S \int_{-\infty}^{\infty} A(t,x)dt \end{aligned} \tag{28}$$

where S is the area of capillary's cross-section.
For the specified variables from equation (27), integration by time in limits from minus infinity to plus infinity give us the following expression for $\mathbf{A}_{\text{free}}$:

$$\mathbf{A}_{\text{free}} = v_{\text{A}} S \int_{-\infty}^{\infty} A(t,x)dt = -\frac{S(v_{\text{B}} - v_{\text{A}})}{k_{\text{on}}} \times$$

$$\times \ln\left\{\exp\left\{k_{\text{on}} \int_{-\infty}^{\infty} B(0,y)dy/(v_{\text{B}} - v_{\text{A}})\right\} \times \left(\exp\left\{\int_{-\infty}^{x-v_A t} A(0,y)dy/(v_{\text{B}} - v_{\text{A}})\right\} - 1\right) + 1\right\}\Bigg|_{t=-\infty}^{t=\infty} = \quad (29)$$

$$= \frac{S(v_{\text{B}} - v_{\text{A}})}{k_{\text{on}}} \ln\left\{\left(\exp\left(k_{\text{on}}\mathbf{A}_{\text{in}}/\left(S(v_{\text{B}} - v_{\text{A}})\right)\right) - 1\right) \times \exp\left(k_{\text{on}}\mathbf{B}_{\text{in}}/\left(S(v_{\text{A}} - v_{\text{B}})\right)\right) + 1\right\}$$

To simplify equation (29) we introduce the following parameters:

$$\varepsilon = k_{\text{on}}\mathbf{A}_{\text{in}}/(S(v_{\text{B}} - v_{\text{A}})) \quad (30)$$

Equation (39) can then be converted into:

$$\mathbf{A}_{\text{free}}/\mathbf{A}_{\text{in}} = \frac{1}{\varepsilon}\ln\left\{\left(\exp(\varepsilon) - 1\right)\exp(-\varepsilon \times \mathbf{B}_{\text{in}}/\mathbf{A}_{\text{in}}) + 1\right\} \quad (31)$$

Finally, when ε is found from (31), k_{on} can be found from rearranged (30):

$$k_{\text{on}} = \varepsilon S(v_{\text{B}} - v_{\text{A}})/\mathbf{A}_{\text{in}} \quad (32)$$

where the velocities are found by dividing the effective capillary length by the corresponding migration time.

4. Correctness of the assumptions

The major assumption of this mathematical model is that the complex formation reaction occurs only when the zone of B moves through that of A, while the dissociation process occurs only after the zones of A and B are separated. To model this we will consider the situation presented in Figure 1 below, where the plugs of components A and B with the lengths l_{A} and l_{B} and velocities v_{A} and v_{B}, respectively, are interacting inside the capillary. It is assumed that the velocity of A is higher than that of B. The velocities of A and B can be presented relative to that of C: $v'_{\text{A}} = v_{\text{A}} - v_{\text{C}}$, $v'_{\text{B}} = v_{\text{B}} - v_{\text{C}}$. For simplicity of mathematical calculations we will set $v_{\text{C}} = 0$.

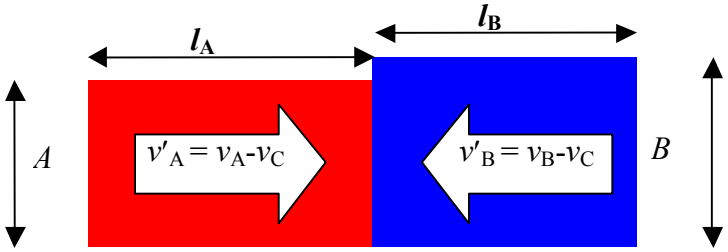

Figure 1. Graphic representations of 2 plugs interacting in the capillary. The heights of the rectangles correspond to concentrations of A and B in the plugs.

In the model above, the rate of complex formation can be described by the equation directly following from system of equations (1):

$$y = x - tv_{\text{C}}$$
$$\frac{dC(t,y)}{dt} = k_{\text{on}} A(t,y)B(t,y) - k_{\text{off}} C(t,y) \quad (33)$$

For simplicity we will assume, that the concentrations of A and B are homogeneous and distributed evenly throughout the length of respective plugs, thus, the concentrations are independent of t and y" $A(t,y) = A$, $B(t,y) = B$.

Assuming that $t << 1/k_{off}$ equation (33) has the following solution:

$$C(t,y) = \frac{k_{on} AB}{k_{off}}(1 - \exp(-tk_{off})) \approx k_{on} ABt \tag{34}$$

The amount of the complex, $C_{diss}(t_{pass},y)$, dissociated during $t = t_{pass}$, where t_{pass} is the time of plugs passing through each other, can be defined for $t_{pass} << 1/k_{off}$ using the Taylor series expansion:

$$C_{diss}(t_{pass}, y) = k_{off} \int_0^{t_{pass}} C(t,y)dt = k_{on} AB(t_{pass} k_{off} - 1 + \exp(-t_{pass} k_{off})) \approx k_{off} k_{on} ABt_{pass}^{\ 2} / 2 \tag{35}$$

t_{pass} will be the smaller of two times, $l_A/(v_C - v_A)$ and $l_B/(v_B - v_C)$, and can be estimated as:

$$t_{pass} = \min(l_A / |v_A - v_C|, l_B / |v_B - v_C|) \tag{36}$$

where function $\min(x,y)$ represents the smallest value out of the two arguments: $l_A/(v_C - v_A)$ and $l_B/(v_B - v_C)$. The value of C_{diss} should be smaller than both concentrations of substrates; otherwise, the distributions of reacted A and B plugs will change significantly due to the dissociation of the complex:

$$k_{off} k_{on} ABt_{pass}^{\ 2} << 2\min(A, B) \tag{37}$$

Condition (37) can be transformed into the following:

$$k_{off} << 2/(k_{on} \max(A, B) t_{pass}^{\ 2}) \tag{38}$$

where function $\max(x,y)$ is the largest value out of two arguments.

We assumed before, that $k_{off} << 1/t_{pass}$. Combining this assumption for k_{off} with assumption (38) will finally give:

$$k_{off} << \min(1, 2/(k_{on} \max(A, B) t_{pass}))/t_{pass} \tag{39}$$

Using formula (39) we generated the table of upper acceptable limits for k_{off} as functions of k_{on}, t_{pass}, and initial concentrations, A and B. This data are presented in the Table 1 in the main text.